Pergamon

Int. J. Solids Structures Vol. 32, No. 11, pp. 1517–1533, 1995

0020–7683/95 $9.50 + .00

0020–7683(94)00231–2

BRITTLE RESPONSE OF CONCRETE AS A LOCALIZATION PROBLEM

S. PIETRUSZCZAK and G. XU
Department of Civil Engineering, McMaster University, Hamilton, Ontario, Canada

(*Received* 2 *March* 1994; *in revised form* 14 *September* 1994)

Abstract—A mathematical formulation for the mechanical response of concrete and similar cemented aggregate mixtures is presented. The stable response, associated with the growth of microcracks, is described by a phenomenological plasticity framework. The transition to unstable response, invoking localized deformation, is considered as a bifurcation problem. In the localized mode, the mechanical behaviour is modelled by estimating, through a homogenization technique, the average mechanical properties of a medium intercepted by a macrocrack. The strain-softening behaviour is the result of unstable response along the interface, triggered by a progressive degradation of surface asperities. The mathematical framework is illustrated by some numerical examples. The strain localization criterion, derived from considerations of stability of the constitutive relation governing the homogeneous deformation mode, is applied to determine the bifurcation point and the orientation of the macrocrack in a series of plane strain tests. The simulations of unstable response are also provided, illustrating the effect of the size of the sample on average mechanical characteristics. The formulation is incorporated in a finite element code to investigate the progressive failure of concrete blocks subjected to uniaxial compression.

INTRODUCTION

The behaviour of plastic-fracturing materials, like cemented aggregate mixtures, has been the object of intensive research over the last few decades. An extensive survey, focusing on constitutive relations, fracture, creep, heat and moisture transfer, can be found in Bazant (1989). The paper, which provides nearly 100 references, identifies the principal advances in all these areas since the early 1970s. Despite many significant contributions, the description of the mechanical response of cemented aggregate mixtures still poses a formidable challenge. In such materials, the deformation process consists initially of nucleation and growth of microcracks. For certain stress paths, however, the subsequent damage may become localized along discrete failure planes (macrocracks). Formation of such a mechanism is usually associated with an unstable material response. The objective of this paper is to outline a simple methodology for describing both stages of the deformation process and to implement the proposed approach in the context of a boundary-value problem.

The work described here is an extension of research reported earlier by Pietruszczak *et al.* (1988). In that reference, a constitutive model for concrete, built within the framework of rate-independent theory of plasticity, has been presented. Although the material description includes the unstable (strain-softening) response, the formulation of the problem is not rigorous. First, the inception of strain-softening, corresponding to formation of a macrocrack, is governed by a path-independent criterion which is imposed *a priori*. Moreover, the mathematical formulation incorporates some empirically-based functions correlating the rate of strain-softening with geometrical aspects. In this paper a more rigorous approach is pursued. The ductile–brittle transition is considered as a bifurcation problem, i.e. loss of stability of the constitutive equation governing the homogeneous deformation. The strain-softening behaviour is attributed to a non-homogeneous mode resulting from macroscopic fracturing and subsequent sliding along asperities. The response in an unstable regime is defined by estimating the average mechanical properties of a heterogeneous medium consisting of an interface (i.e. macrocrack) and the adjacent intact material.

In the next section, a constitutive model for the description of distributed damage, associated with a stable response, is briefly outlined. The formulation is then applied to investigate the inception of strain localization, i.e. formation of a macrocrack. Numerical

examples include the simulation of a series of plane strain uniaxial compression tests performed at different initial confining pressures. In particular, the sensitivity of the ductile–brittle transition and that of the orientation of the macrocrack to the initial test conditions are investigated. The predicted qualitative trends are consistent with the existing experimental data (Palaniswamy and Shah, 1974). In the subsequent sections, the homogenization technique for dealing with localized deformation mode is first reviewed [after Pietruszczak and Niu (1993)], followed by a presentation of a constitutive model for the interface. The formulation is later applied to study the average response of non-homogeneous samples in an unstable regime. Finally, the proposed approach is implemented in the context of a boundary-value problem. In particular, the finite element analysis of the progressive failure of concrete blocks loaded in compression is performed.

DESCRIPTION OF STABLE RESPONSE OF CONCRETE

The constitutive model employed in this study is based on the phenomenological plasticity framework proposed by Pietruszczak *et al.* (1988). The formulation invokes the concept of a failure locus which is introduced *a priori* as a path-independent criterion. The deformation process is described in terms of evolution of the family of yield surfaces $f(\sigma_{ij}, \xi) = 0$, where ξ is a suitably chosen damage parameter. The direction of plastic flow is determined from a non-associated flow rule, which involves the existence of a family of plastic potential surfaces defined in a parametric form, $\Psi(\sigma_{ij}) = \text{const}$. The formulation outlined here is restricted to a stable (strain-hardening) deformation mode only. The transition to unstable behaviour is considered later within the context of bifurcation analysis.

The failure locus is chosen in the form

$$F = \bar{\sigma} - g(\theta)\bar{\sigma}_c = 0 \tag{1}$$

where

$$\bar{\sigma}_c = \frac{-a_1 + \sqrt{(a_1^2 + 4a_2(a_3 + I/f_c))}}{2a_2} f_c. \tag{2}$$

In the above equations $I = -\sigma_{ii}$, $\bar{\sigma} = (1/2\ s_{ij}s_{ij})^{1/2}$, $\theta = 1/3\ \sin^{-1}(3\sqrt{3}J_3/2\bar{\sigma}^3)$ and $J_3 = 1/3\ s_{ij}s_{jk}s_{ki}$ are the stress invariants. Moreover, the parameters a_1, a_2 and a_3 represent dimensionless material constants and f_c denotes the uniaxial compressive strength of concrete. It should be noted that in the principal stress space, eqn (1) describes an irregular cone with smooth curved meridians and a non-circular convex cross-section, defined by $g(\theta)$. The functional form of $g(\theta)$ is assumed to be affected by the value of confining pressure. A number of possible representations for this function have been provided by Jiang and Pietruszczak (1988).

The yield surface is chosen in a functional form similar to that of eqn (1), i.e.

$$f = \bar{\sigma} - \beta(\xi)g(\theta)\bar{\sigma}_c = 0, \tag{3}$$

where $\beta(\xi)$ represents a hardening function. The internal variable ξ is related to the history of accumulated plastic distortions,

$$\xi = \int d\xi; \quad d\xi = (de_{ij}^p\, de_{ij}^p)^{1/2}/\bar{\Phi}, \tag{4}$$

where de_{ij}^p represents the deviatoric part of the plastic strain rate and $\bar{\Phi} = \text{const.}$ is defined through an appropriate parametric equation $\bar{\Phi} = \Phi(I, \theta)$ [see Pietruszczak *et al.* (1988)].

The direction of plastic flow is governed by a non-associated flow rule and the corresponding plastic potential is selected in the form

$$\Psi = \bar{\sigma} + m_c g(\theta)\bar{I}\ln(\bar{I}/\bar{I}_0) = 0. \tag{5}$$

In eqn (5), m_c represents the value of $m = \bar{\sigma}/(g(\theta)\bar{I})$ for which $d\varepsilon_{ii}^p = 0$ (i.e. a transition from compaction to dilatancy takes place), whereas $\bar{I} = a_0 f_c + I$ and a_0 defines the location of the apex of the current potential surface in the tensile domain.

Finally, the hardening function may be chosen in a simple hyperbolic form:

$$\beta = \xi/(A+\xi), \tag{6}$$

where A is a material constant. According to eqn (6), for $\xi \to \infty$ there is $\beta(\xi) \to 1$, which implies that the yield surface asymptotically approaches the failure surface.

TRANSITION TO BRITTLE RESPONSE AS A BIFURCATION PROBLEM

The growth of microcracks is a fairly distributed process which is associated with a stable material response. For certain stress trajectories, however, a different deformation mode may prevail, consisting of formation of discrete failure planes (macrocracks). In the latter case, the mechanical response as observed on the macroscale becomes, in general, unstable. The inception of a localized mode may be considered as a bifurcation problem, i.e. loss of stability of the constitutive relation governing the homogeneous deformation. The conditions under which localized modes arise have been investigated by a number of researchers. Preference has been given to study the shear band formation in ductile materials like metals or soils (Rudnicki and Rice, 1975) and only limited research has been conducted in the context of brittle materials (Ortiz, 1987). Some of the basic principles underlying the theory follow from early studies on elastic stability, later extended to inelastic materials (Hill, 1958; Thomas, 1961). A detailed review of the subject can be found, for example, in Bardet (1990).

Consider a homogeneous sample, under a uniform stress field σ_{ij}, subjected to a quasi-static strain rate $\dot{\varepsilon}_{ij}$. The deformation field within the sample will, in general, remain uniform; in some cases, however, a bifurcation may occur in such a manner that the subsequent deformation becomes discontinuous across a plane of orientation n_i. For a small deformation theory, the condition for the inception of strain localization takes the form (Rudnicki and Rice, 1975)

$$\det B_{jk} = 0; \quad B_{jk} = n_i D_{ijkl} n_l, \tag{7}$$

where D_{ijkl} is the constitutive tensor governing the homogeneous deformation mode. In numerical terms, the problem reduces to a constrained minimization problem for $f(n_i) = \det B_{jk}$ under $n_i n_i = 1$, where n_i can be expressed in terms of two spherical angles defining the orientation of the shear band.

The above approach has been applied to study the onset of localization using the constitutive model summarized in the previous section. In particular, a series of plane strain uniaxial compression tests have been simulated assuming the following set of material parameters:

$$E = 35{,}000\,\text{MPa}, \quad \nu = 0.20, \quad f_c = 50\,\text{MPa}, \quad f_t = 5\,\text{MPa}, \quad A = 0.000085.$$

The main objective was to investigate the sensitivity of the inception of localized damage to the value of the initial confining pressure I_0. The constitutive relation for concrete has been integrated using the forward-Euler explicit algorithm and imposing mixed boundary conditions, i.e. $\dot{\varepsilon}_{22} < 0$ ($\dot{\varepsilon}_{i3} = 0, i = 1, 2, 3$) under $\dot{\sigma}_{11} = 0$. At each integration step the constitutive matrix D_{ijkl} was computed and the localization condition (7) checked.

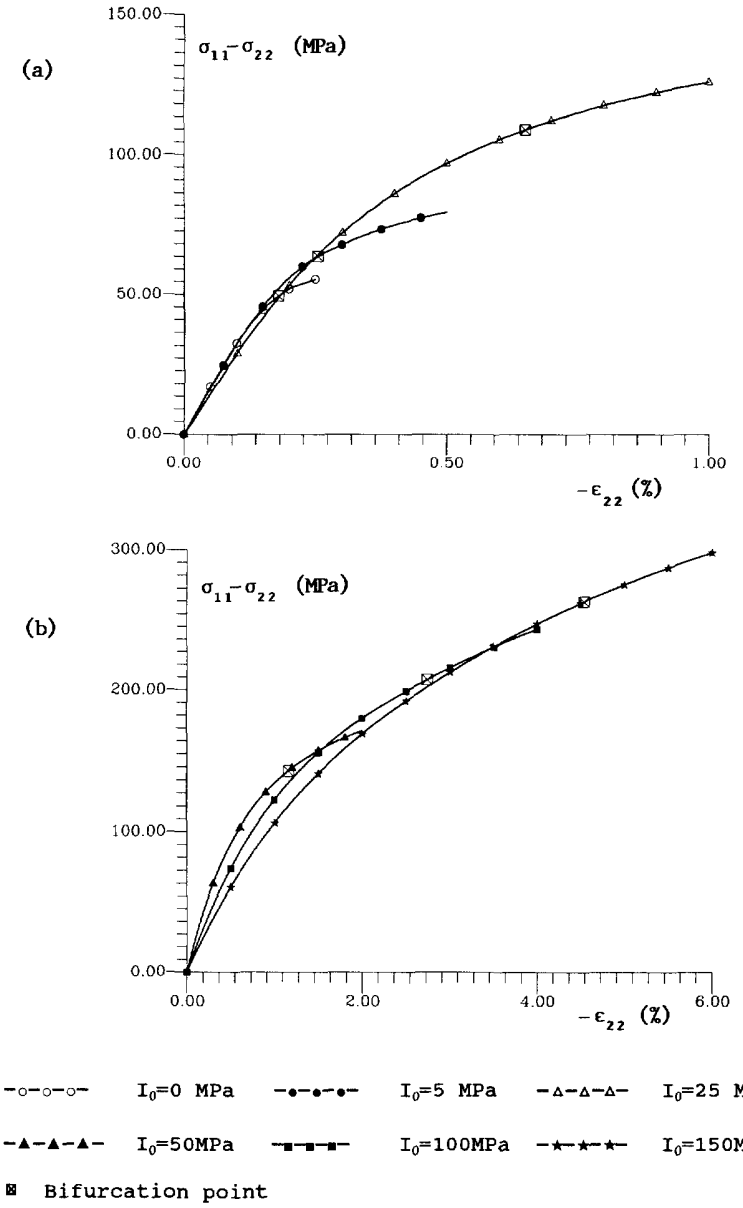

Fig. 1. Numerical simulations of a ductile–brittle transition in plane strain uniaxial compression.

The results are presented in Fig. 1, which shows the deviatoric characteristics corresponding to confining pressures ranging from 0 to 150 MPa. At the same time, Table 1 gives the numerical details pertaining to the detection of the bifurcation point and the orientation of the failure plane. At low initial confining pressures, $0 < I_0 < 25$ MPa, the transition to localized mode takes place at axial strain intensities within the range of 0.5%. As the confining pressure increases, the stable mode associated with formation and growth of microcracks becomes predominant. At high pressures, $I_0 > 100$ MPa, the discrete failure planes can only form at strain levels which are practically not attainable in the context of typical boundary value problems, implying that the failure mode involves primarily the distributed damage (Fig. 1b). The initial conditions also affect the orientation of the failure plane. In particular, the inclination of this plane with respect to the major principal stress progressively decreases with increasing confining pressure.

Table 1. Results of bifurcation analysis for plane strain uniaxial compression tests

Initial confining pressure I_0 (MPa)	Inclination of shear band (β)	Bifurcation point $-\varepsilon_{22}$ (%)	Bifurcation point $\sigma_{11}-\sigma_{22}$ (MPa)
0	56.2	0.18	49.38
5	54.2	0.26	63.63
25	50.0	0.65	108.71
50	48.0	1.16	142.61
100	46.5	2.74	207.21
150	45.5	4.54	263.10

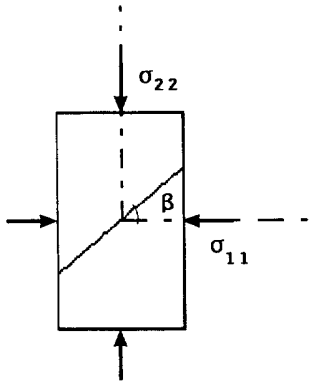

DESCRIPTION OF LOCALIZED DAMAGE

In a large class of boundary value problems the loss of stability of a structure occurs soon after the initiation of localized damage. The propagation of this damaged zone, which in itself leads to formation of a distinct failure mechanism, requires very little mechanical effort, so that the ultimate load differs only marginally from that corresponding to the onset of localization. In this case, the bifurcation analysis alone may be sufficient to estimate the critical intensity of external load. In some structural problems, however, the loss of stability is associated with a "diffused" mode of failure involving formation of local shear bands (macrocracks), which eventually collapse into a discrete set of failure planes triggering the overall loss of stability of the structure. In the latter case, the ultimate load is significantly affected by characteristics in the post-localized stage, which are usually associated with unstable material behaviour. Therefore, an appropriate description of these characteristics is essential for a reliable solution of the above mentioned class of problems.

It is well known that standard rate-independent continuum theories cannot adequately model the localized damage. In a typical formulation, the measured force–displacement response is simply converted to a stress–strain relation, ignoring the inhomogeneous nature of the deformation process. As a result, the material parameters cannot be uniquely determined since the experimental response depends explicitly on the geometry of the specimen. In mathematical terms, the elliptic character of the set of governing differential equations is lost and the numerical analysis suffers from spurious mesh sensitivity.

In order to overcome these deficiencies the classical continuum formulations have been enriched by incorporating additional terms which signify the evolution of microstructure associated with the localized damage. In the last decade several conceptually different approaches for modelling of localized deformation have emerged, including the use of micro-polar continua (Muhlhaus and Vardoulakis, 1987; de Borst, 1991, 1993), non-local theories (Pijaudier-Cabot and Bazant, 1987), gradient-dependent formulations (Aifantis, 1984; Muhlhaus and Aifantis, 1991; de Borst and Muhlhaus, 1992), etc. In a Cosserat continuum the generalized stress–strain components include couple-stresses and micro-curvatures. The formulation incorporates an internal length scale, rendering the numerical solutions to be virtually independent of the details of discretization. A significant advantage of this formulation, as compared to other non-standard approaches, is that the framework can be implemented in finite element algorithms using standard plasticity procedures for

deriving the tangent operators. A distinct drawback is the fact that the rotational degrees of freedom cannot be activated in pure tension. Consequently, for problems in which mode I failure is the predominant mechanism, the analysis may still suffer from deficiencies pertinent to classical models. In gradient theories, which may be considered as a sub-set of non-local theories, the functional form of the yield surface incorporates higher order gradients of inelastic strain. While non-local models require special numerical strategies, the gradient formulations are computationally more efficient (de Borst and Muhlhaus, 1992). Both these formulations, however, invoke non-standard boundary conditions. The presence of an internal length scale, once again, ensures that the solutions are not affected by the discretization and thus remain objective in the numerical sense. One of the major problems when dealing with higher-order continua (as well as Cosserat media) is the question of identification of material parameters. In general, the parameters cannot be measured or derived from elementary material tests, which is largely due to the phenomenological structure of these formulations. The only alternative seems to be the fitting of experimental results by means of numerical analyses. This, however, is not only inefficient but also quite ambiguous, particularly in the case when a number of material parameters is involved. A similar problem arises in the context of a viscoplastic regularization, whereby it is difficult to differentiate between the effects of rate sensitivity of the material itself and the influence of the inertia forces in the context of a coupled dynamic analysis.

The approach followed here is based on estimating, through a simple homogenization technique, the average mechanical properties in the domain adjacent to the region undergoing localized damage. Such a description has been originally proposed within the context of soil mechanics (Pietruszczak and Mroz, 1981) and later modified and implemented in the finite element analysis of some geotechnical problems (Pietruszczak and Niu, 1993). The formulation may be considered as an alternative non-standard continuum approach. It incorporates an additional parameter, which has the dimension of length and is identified with the ratio of the area of the homogenized domain to the length of the localized zone penetrating this domain (in a two-dimensional context). The thickness of the localized zone, which is a multiple of the mean aggregate size, has no direct effect on the global response. There is an explicit distinction between the mechanical properties in the intact and localized region (not present in other continuum formulations). Consequently, the averaged response is a function of the properties of both constituent materials, the latter identifiable form elementary material tests, as pointed out later in this paper. From a numerical viewpoint, no special techniques are required for implementation in a finite element algorithm and no direct restrictions are placed on the discretization scheme (Pietruszczak and Niu, 1993). The main disadvantage is the simplicity of the homogenization procedure itself, which is based on rather restrictive assumptions. There is also an element of ambiguity in estimating the characteristic length parameter in the context of a finite element discretization (the precise location of the shear band is unknown). Such an ambiguity, however, is even more pronounced in the context of the definition (and estimates) of the internal length scale introduced in other non-standard continuum formulations. In what follows, the main aspects of the averaging procedure are briefly summarized and the formulation is subsequently applied to study the phenomenon of localized damage in concrete.

Consider a volume of the material adjacent to a narrow shear band (interface) which intercepts this region. Let $\dot{\boldsymbol{\sigma}}^{(i)}$, $\dot{\boldsymbol{\varepsilon}}^{(i)}$ $(i = 1, 2)$ denote the average stress–strain rates in the constituents involved, i.e. the intact material and the medium confined to the shear band. Both of these tensorial fields are considered to be homogeneous within themselves. If the constituents are perfectly bonded then the integration over the volume of an representative element yields (Hill, 1963)

$$\dot{\boldsymbol{\sigma}} = \mu_1 \dot{\boldsymbol{\sigma}}^{(1)} + \mu_2 \dot{\boldsymbol{\sigma}}^{(2)}; \quad \dot{\boldsymbol{\varepsilon}} = \mu_1 \dot{\boldsymbol{\varepsilon}}^{(1)} + \mu_2 \dot{\boldsymbol{\varepsilon}}^{(2)}, \tag{8}$$

where $\dot{\boldsymbol{\sigma}}$ is the applied stress rate, $\dot{\boldsymbol{\varepsilon}}$ is resulting average macroscopic deformation of the composite body and $\mu_i (i = 1, 2)$ are the respective volume fractions. It should be emphasized

that $\boldsymbol{\sigma}^{(i)}$ and $\boldsymbol{\varepsilon}^{(i)}$ refer to the *macroscopic* stress and deformation of the constituents and are not intended as measures of the deformation process at the microscopic level. For the discussion that follows, eqns (8) are supplemented by a set of kinematic and static constraints:

$$k_j(\dot{\boldsymbol{\varepsilon}}^{(1)}, \dot{\boldsymbol{\varepsilon}}^{(2)}) = 0; \quad s_j(\dot{\boldsymbol{\sigma}}^{(1)}, \dot{\boldsymbol{\sigma}}^{(2)}) = 0, \tag{9}$$

where k and s are scalar-valued functions and j specifies the number of constraints. Equations (8) and (9), together with the corresponding constitutive relations, form a set of differential equations which is complete, i.e. the response of the composite is uniquely defined in terms of properties of constituents and respective volume fractions. It should be noted that constraints (9), which are frequently used to estimate the properties of fibre-reinforced (Dvorak and Bahei-El-Din, 1982) and layered composites (Sawicki, 1983), are restrictive. Rigorous formulation requires, in general, that the kinematic compatibility and static constraints be specified in terms of velocities and traction along the interface between the constituents. This is a rather strong assumption which has to be eventually relaxed in order to render a feasible solution.

Within the context of an inhomogeneity in the form of a narrow shear band, constraints (9) can be expressed in the form

$$\dot{\varepsilon}_{11} = \dot{\varepsilon}_{11}^{(1)} = \dot{\varepsilon}_{11}^{(2)}; \quad \dot{\varepsilon}_{33} = \dot{\varepsilon}_{33}^{(1)} = \dot{\varepsilon}_{33}^{(2)}; \quad \dot{\gamma}_{13} = \dot{\gamma}_{13}^{(1)} = \dot{\gamma}_{13}^{(2)}$$

$$\dot{\sigma}_{22} = \dot{\sigma}_{22}^{(1)} = \dot{\sigma}_{22}^{(2)}; \quad \dot{\sigma}_{12} = \dot{\sigma}_{12}^{(1)} = \dot{\sigma}_{12}^{(2)}; \quad \dot{\sigma}_{23} = \dot{\sigma}_{23}^{(1)} = \dot{\sigma}_{23}^{(2)}. \tag{10}$$

Here the coordinate system has been chosen in such a way that the x_2-axis is along the normal to the shear band and $\dot{\boldsymbol{\varepsilon}}$ is defined as $\dot{\boldsymbol{\varepsilon}} = \{\dot{\varepsilon}_{11}, \dot{\varepsilon}_{22}, \dot{\varepsilon}_{33}, \dot{\gamma}_{12}, \dot{\gamma}_{13}, \dot{\gamma}_{23}\}^{\mathrm{T}}$. The thickness of the shear band (say, 10 times the mean aggregate size) may be considered as negligible compared to other physical dimensions involved. Thus, it can formally be eliminated from *macroscopic* considerations by expressing the local deformation field in terms of velocity discontinuities $\dot{\mathbf{g}}$ rather than strain rates $\dot{\boldsymbol{\varepsilon}}^{(2)}$. Denoting $\dot{\mathbf{g}}$ as $\dot{\mathbf{g}} = \{\dot{g}_2, \dot{g}_1, \dot{g}_3\}^{\mathrm{T}}$, where $\dot{g}_2$ is the normal component and $\dot{g}_1$ and $\dot{g}_3$ the tangential components of the velocity discontinuity, the strain decomposition in eqn (8) reduces to

$$[\delta]\dot{\boldsymbol{\varepsilon}} = [\delta]\dot{\boldsymbol{\varepsilon}}^{(1)} + \mu\dot{\mathbf{g}}, \tag{11}$$

where

$$[\delta] = \begin{bmatrix} 0 & 1 & 0 & 0 & 0 & 0 \\ 0 & 0 & 0 & 1 & 0 & 0 \\ 0 & 0 & 0 & 0 & 0 & 1 \end{bmatrix}.$$

In eqn (11), μ defines the ratio of the cross-sectional area of the failure plane to the volume of the representative element. Thus, μ^{-1} has the dimension of length and may be considered as a characteristic length parameter. Writing now the constitutive relations, for both constituents involved, in the form

$$\dot{\boldsymbol{\sigma}}^{(1)} = [D]\dot{\boldsymbol{\varepsilon}}^{(1)}; \quad \dot{\boldsymbol{\sigma}}^{(2)} = [K]\dot{\mathbf{g}}, \tag{12}$$

it is apparent that the problem is mathematically determinate. Indeed, the stress decomposition in eqn (8), together with eqns (10)–(12), provide the set of 27 equations for 27 unknowns. The solution can be expressed as

$$\dot{\boldsymbol{\sigma}} \approx [D][S_1]\dot{\boldsymbol{\varepsilon}}; \quad \dot{\boldsymbol{\varepsilon}}^{(1)} = [S_1]\dot{\boldsymbol{\varepsilon}}; \quad \dot{\mathbf{g}} = [S_2]\dot{\boldsymbol{\varepsilon}}, \tag{13}$$

where the components of $[S_1]$ and $[S_2]$ are function of the parameter μ and properties of

the materials involved. An explicit definition of both of these matrices is provided in Pietruszczak and Niu (1993).

The implementation of the above framework requires the description of mechanical characteristics of the material confined to the shear band. Ideally, such characteristics should be derived from micromechanical considerations, taking into account a progressive evolution of the geometry of the microstructure. As an illustration, a simple constitutive model, based on the physical framework proposed by Dowding *et al.* (1991), is presented in the next section. It should be pointed out that the material parameters associated with constitutive relations (12), and thus (13), are identifiable from elementary material tests. An extended discussion on identification of properties of the intact material is provided in Pietruszczak *et al.* (1988). The material characteristics of the interface can also be measured experimentally. Perhaps the most appropriate procedure is to fail initially homogeneous samples in mode I and subsequently identify the interface properties from a series of direct shear tests performed at different normal stress intensities.

CONSTITUTIVE MODEL FOR THE INTERFACE

Assume that the deformation in the neighbourhood of the interface results from sliding along a set of asperities, with a pre-defined orientation, coupled with a progressive degradation of these asperities. The sliding process is described by invoking the classical elastic–perfectly plastic formulation, whereas the degradation phenomenon, attributed to accumulated discontinuities in tangential components of velocity, reduces asperities' inclination and results in an unstable strain-softening response.

In general, the interface surface may be very irregular so that a significant bias in the spatial distribution of asperities orientation occurs. Such a bias can be described by employing the mathematical representation analogous to that in Pietruszczak and Krucinski (1989), i.e. defining the "directional" distribution of asperities orientation as an average, continuous measure expressed in terms of an expansion based on symmetric traceless tensors. In this section, a very simple conceptual framework, similar to that of Dowding *et al.* (1991), will be discussed based on a rather drastic geometric idealization. Firstly, the formulation will be restricted to a two-dimensional case, in which out-of-plane motion is not accounted for. Secondly, the interface surface will be idealized as consisting of a set of sawtooth asperities with a uniform (in an average sense) inclination α with respect to the direction of the interface. Since the orientation is said to be uniform and the sliding process is governed by the ratio of normal and tangential components of the resultant force acting along each asperity, the formulation becomes invariant with respect to the number of active asperities and the actual contact areas between them. Thus, the problem can be reduced to considering the deformation resulting from sliding along a single "representative" asperity. Note that the orientation of this asperity, defined by α, may in general be different for sliding in two opposite directions.

Given the above assumptions, consider now the deformation process in the neighbourhood of the idealized interface. Introduce a local frame of reference $\bar{\mathbf{x}}$, such that the $\bar{x}_2$-axis is along the normal to the asperity. If $\mathbf{F} = \{F_2, F_1\}^T$ is the resultant force acting at the interface, then

$$\mathbf{F} = [T]\bar{\mathbf{F}}; \quad [T] = \begin{bmatrix} \cos\alpha & \sin\alpha \\ -\sin\alpha & \cos\alpha \end{bmatrix}, \tag{14}$$

where $\bar{\mathbf{F}} = \{\bar{F}_2, \bar{F}_1\}^T$ is the force transmitted through the asperity of orientation α. A similar transformation law applies to the displacement discontinuity vector $\mathbf{g} = \{g_2, g_1\}^T$. The sliding along the asperity is described in terms of an elastic–perfectly plastic formulation, in which the yield and plastic potential functions are selected as

$$f(\bar{\mathbf{F}}) = |\bar{F}_1| + \eta \bar{F}_2 = 0; \quad Q = |\bar{F}_1| = \text{const}, \tag{15}$$

with $\eta = \text{const}$. The consistency condition reads

$$\dot{f} = \left(\frac{\partial \mathrm{f}}{\partial \bar{\mathbf{F}}}\right)^{\mathrm{T}} \dot{\bar{\mathbf{F}}} = 0; \quad \dot{\bar{\mathbf{F}}} = [T]^{\mathrm{T}} \dot{\mathbf{F}} + \left(\frac{\partial}{\partial \alpha}[T]^{\mathrm{T}}\right) \mathbf{F} \dot{\alpha}. \tag{16}$$

Assume now that the flow rule and the evolution law for the asperity orientation take the form

$$\dot{\bar{\mathbf{g}}}^{\mathrm{p}} = \dot{\lambda} \frac{\partial Q}{\partial \bar{\mathbf{F}}}; \quad \alpha = \alpha(\bar{g}_1^{\mathrm{p}}). \tag{17}$$

Since, according to eqn (17), the degradation of asperities is affected only by irreversible deformations, the response in the elastic range can be defined as

$$\dot{\mathbf{F}} = [k^{\mathrm{e}}](\dot{\mathbf{g}} - \dot{\bar{\mathbf{g}}}^{\mathrm{p}}); \quad [k^{\mathrm{e}}] = \begin{bmatrix} k_{\mathrm{N}} & 0 \\ 0 & k_{\mathrm{T}} \end{bmatrix}, \tag{18}$$

where k_{N} and k_{T} represent the normal and shear stiffnesses, respectively.
Substituting eqns (18) and (17) in the consistency condition (16) and noting that

$$\dot{\alpha} = \frac{\partial \alpha}{\partial \bar{g}_1^{\mathrm{p}}} SIG(\bar{F}_1)\dot{\lambda}; \quad \dot{\bar{\mathbf{g}}}^{\mathrm{p}} = [T]\dot{\bar{\mathbf{g}}}^{\mathrm{p}} + \left(\frac{\partial}{\partial \alpha}[T]\right)\bar{\mathbf{g}}^{\mathrm{p}}\dot{\alpha}, \tag{19}$$

one obtains, after some transformations

$$\dot{\lambda} = \left(\frac{\partial f}{\partial \bar{\mathbf{F}}}\right)^{\mathrm{T}} [T]^{\mathrm{T}}[k^{\mathrm{e}}]\dot{\mathbf{g}}/H, \tag{20}$$

where

$$H = H_1 + H_2; \quad H_1 = \left(\frac{\partial f}{\partial \bar{\mathbf{F}}}\right)^{\mathrm{T}} [T]^{\mathrm{T}}[k^{\mathrm{e}}][T]\frac{\partial Q}{\partial \bar{\mathbf{F}}}$$

$$H_2 = \left(\frac{\partial f}{\partial \bar{\mathbf{F}}}\right)^{\mathrm{T}} [T]^{\mathrm{T}}[k^{\mathrm{e}}]\left(\frac{\partial}{\partial \alpha}[T]\right)\bar{\mathbf{g}}^{\mathrm{p}}\frac{\partial \alpha}{\partial \bar{g}_1^{\mathrm{p}}} SIG(\bar{F}_1) - \left(\frac{\partial f}{\partial \bar{\mathbf{F}}}\right)^{\mathrm{T}}\left(\frac{\partial}{\partial \alpha}[T]^{\mathrm{T}}\right)\mathbf{F}\frac{\partial \alpha}{\partial \bar{g}_1^{\mathrm{p}}} SIG(\bar{F}_1). \tag{21}$$

It should be noted that since $\partial \alpha / \partial g_1^{\mathrm{p}} < 0 \Rightarrow H_2 < 0$, which leads to a locally unstable material response. Following now a standard plasticity procedure, i.e. substituting eqns (17), (19) and (20) into eqn (18) and rearranging, one obtains

$$\dot{\mathbf{F}} = [k]\dot{\mathbf{g}}; \quad [k] = [k^{\mathrm{e}}] - \frac{[k^{\mathrm{e}}]\left([T]\dfrac{\partial Q}{\partial \bar{\mathbf{F}}} + \dfrac{\partial}{\partial \alpha}[T]\bar{\mathbf{g}}^{\mathrm{p}}\dfrac{\partial \alpha}{\partial \bar{g}_1^{\mathrm{p}}} SIG(\bar{F}_1)\right)\left(\dfrac{\partial f}{\partial \bar{\mathbf{F}}}\right)^{\mathrm{T}}[T]^{\mathrm{T}}[k^{\mathrm{e}}]}{H}, \tag{22}$$

where $[k]$ is the elastoplastic stiffness ($\det[k] < 0$) whose components are defined, in explicit terms, as

$$k_{11} = k_N - \frac{k_N^2}{H}(\eta \cos\alpha\, SIG(\bar{F}_1) + \sin\alpha)\left(\sin\alpha + g_1^p \frac{\partial\alpha}{\partial \bar{g}_1^p}\right);$$

$$k_{12} = -\frac{k_N k_T}{H}(-\eta \sin\alpha\, SIG(\bar{F}_1) + \cos\alpha)\left(\sin\alpha + g_1^p \frac{\partial\alpha}{\partial \bar{g}_1^p}\right);$$

$$k_{21} = -\frac{k_N k_T}{H}(\eta \cos\alpha\, SIG(\bar{F}_1) + \sin\alpha)\left(\cos\alpha - g_2^p \frac{\partial\alpha}{\partial \bar{g}_1^p}\right);$$

$$k_{22} = k_T - \frac{k_T^2}{H}(-\eta \sin\alpha\, SIG(\bar{F}_1) + \cos\alpha)\left(\cos\alpha - g_2^p \frac{\partial\alpha}{\partial \bar{g}_1^p}\right). \tag{23}$$

Finally, the degradation law for the orientation of asperities (17) may be assumed in a simple exponential form

$$\alpha = \alpha_0 \exp(-C\bar{g}_1^p), \tag{24}$$

where α_0 is the initial orientation and C represents a material constant.

The constitutive law, presented above, relates the material rates of the resultant force acting at the interface to that of the displacement discontinuity. It is quite apparent that, given the unit cross-sectional area of the interface, eqn (22) can be expressed in the functional form consistent with eqn (12), thereby completing the mathematical formulation of the problem.

In order to provide an illustration, the above described constitutive framework has been applied to simulate the results of a series of direct shear tests as reported by Schneider (1976). The tests have been conducted on hard-formed gypsum samples displaying natural joint morphology typical of a tension joint in granite. Based on the experimental data, the following material parameters have been selected:

$$\eta = 0.82; \quad K_T = 40{,}000\ \mathrm{MN\,m^{-3}}; \quad K_N = 50{,}000\ \mathrm{MN\,m^{-3}},$$

where K_T and K_N represent the elastic stiffnesses (in the tangential and normal directions, respectively) defined according to representation (12). The average inclination of the asperities was estimated [based on surface profiles provided in Schneider (1976)] as $\alpha = 9°$, whereas $C = 25\ \mathrm{m^{-1}}$ was chosen to obtain the best fit approximation to the experimental characteristics.

The results of numerical simulations are presented in Fig. 2. Figure 2a shows the shear stress–deformation curves corresponding to two different values of normal stress, whereas Fig. 2b gives the respective dilatancy profiles. The predictions appear to be in reasonable agreement with the experimental data, particularly in the context of load–deformation characteristics. It is interesting to note that, in the present formulation, the dilation reduces progressively to zero as the asperities degrade. On the other hand, if the convective term in the expression for the velocity discontinuity (19) is dropped, which is equivalent to referring the flow rule to the global frame of reference $\mathbf{x}$, then the dilation approaches a constant value. This is shown in Fig. 3, which provides the respective volumetric characteristics. For both the cases, the shear characteristics (shown in Fig. 2a) remain identical.

NUMERICAL EXAMPLE

The complete mathematical formulation has now been applied to extend the predictions of plane strain uniaxial compression tests (Fig. 1) to the post-localized regime. The simulations have been carried out assuming the following set of interface parameters:

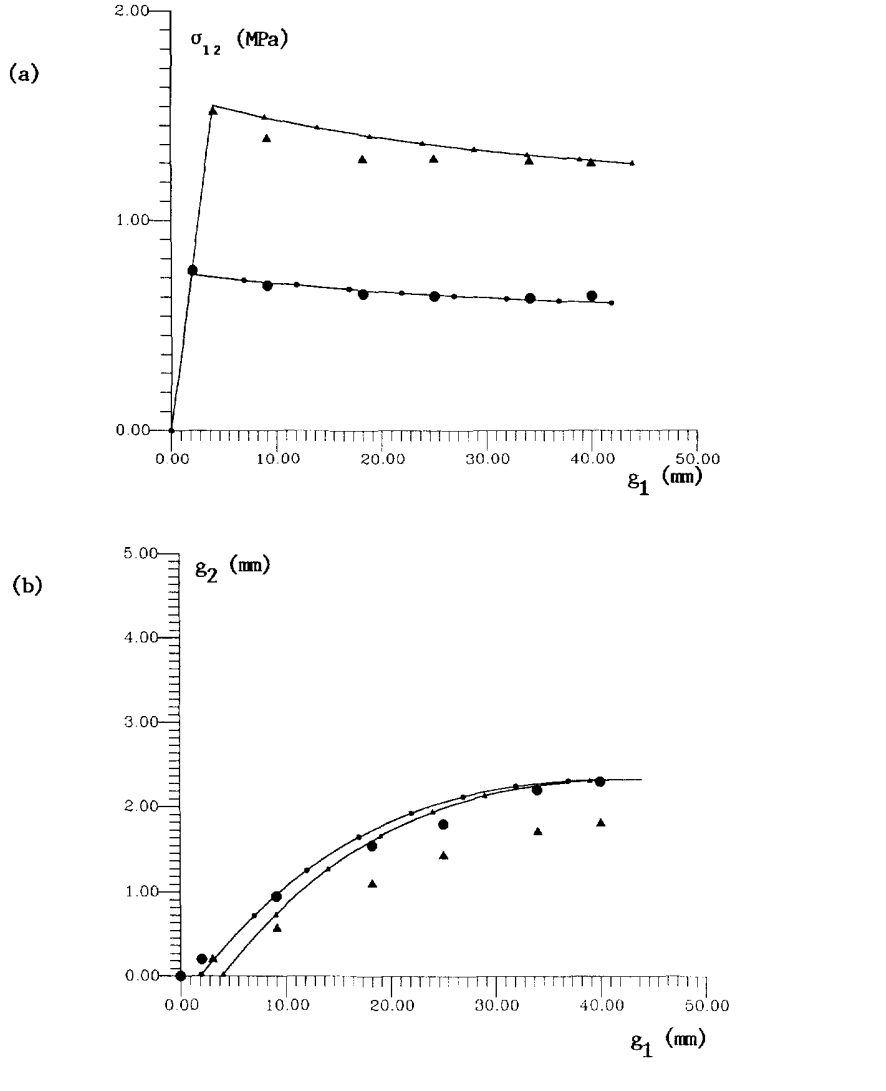

Fig. 2. Response of hard-formed gypsum joints subjected to direct shear.

$$K_T = 40{,}000\,\mathrm{MN\,m^{-3}};\quad K_N = 50{,}000\,\mathrm{MN\,m^{-3}};\quad \alpha = 10^{\circ};\quad C = 200\,\mathrm{m^{-1}}.$$

The above choice is rather arbitrary as no adequate experimental data are available. Thus, the objective here is to investigate the qualitative trends of the response as predicted by the present formulation. It should be noted that the constant η, eqn (15), is not explicitly required here since its value is determined from the bifurcation analysis.

The use of the homogenization technique, eqn (13), implies that the macroscopic response of the sample is sensitive to the parameter μ, defined in eqn (11). In the context of plane strain configuration, μ assumes the value $\mu = (h\cos\beta)^{-1}$, where h is the height of the sample and β defines the orientation of the interface. Thus, even though the macroscopic response is invariant with respect to the thickness of the interface, it depends explicitly on the height of the sample. It should be pointed out that the interface (macrocrack), once formed, constitutes a physical plane of weakness within the intact material. Thus, its orientation is assumed to be fixed upon the onset of localization. This does not preclude

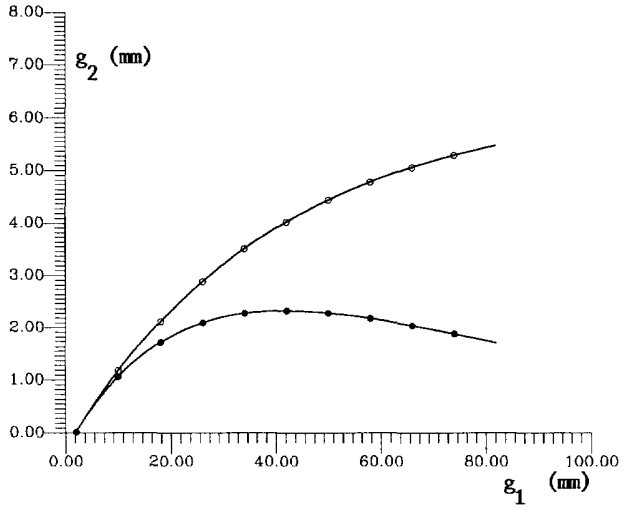

Fig. 3. Influence of the convective term in the expression for the velocity discontinuity on the volumetric characteristics.

the possibility that for deformation histories experiencing large stress reversals additional macrocracks may develop within the same representative volume.

The results of numerical analyses are presented in Figs 4 and 5. Figure 4 shows the mechanical characteristics obtained for a sample of $h = 0.1$ m. The rate of strain softening (Fig. 4a) is virtually insensitive to the confining pressure. This is a rather debatable issue; it should be noted, however, that such a sensitivity, if indeed present, can easily be accounted for by a simple modification of the degradation law (24) (e.g. assuming that the value of C is affected by F_2). Overall, the qualitative aspects, including the nature of volumetric profiles, appear to be consistent with the experimental data provided in Elfgren (1990). Finally, Fig. 5 presents the mechanical characteristics for two samples of $h = 0.1$ m and $h = 0.2$ m subjected to the same loading history. As expected, the response in the post-localized regime is quite sensitive to the geometry of the sample. In particular, the average rate of strain-softening progressively increases with the height of the specimen. The deformation mode, as observed macroscopically, is strongly anisotropic, i.e. the reduction in the vertical stress is accompanied by significant distortions, which is evident from Fig. 5c.

IMPLEMENTATION IN FINITE ELEMENT ANALYSIS

The problem addressed in this section involves the analysis of progressive failure of concrete blocks subjected to uniaxial compression under plane strain conditions. The objective is to analyse the mode of failure as a function of the geometry of specimens. Three blocks, 5 m in width and 5, 7.5 and 10 m high, respectively, have been considered. The loading process consisted of applying uniform vertical displacements along the upper surface under the condition of perfect bonding at the end platens. The specimens were discretized using four-noded rectangular elements (100, 150 and 200 elements, respectively) with isoparametric formulation and 2×2 Gauss quadrature. The material parameters selected for the analysis were identical to those used for numerical simulations discussed in the previous section. The dimension μ, eqn (11), was estimated based on a partitioning rule, after Pietruszczak and Niu (1993). In spite of the symmetry in boundary conditions, the whole structure was discretized in order to verify the criterion for the selection of the shear band orientation [as suggested in Pietruszczak and Niu (1993)]. The problem was solved using the "tangential stiffness" approach (Owen and Hinton, 1980) and employing a non-symmetric equation solver. Since the analysis incorporating the homogenization

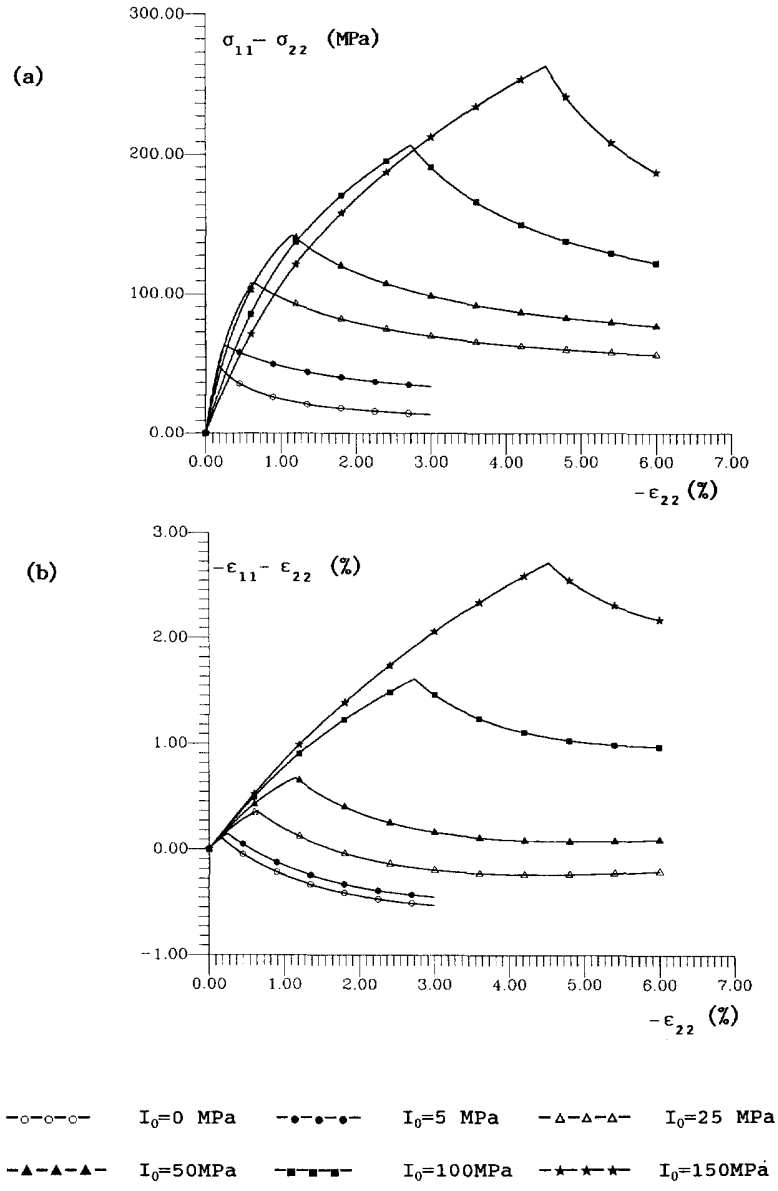

Fig. 4. Numerical simulations of unstable response for a series of plane strain uniaxial compression tests.

procedure, eqn (13), shows little sensitivity to the mesh design, no explicit mesh convergence study was performed.

The results of numerical simulations are shown in Figs 6 and 7. Figure 6 presents the global load–displacement characteristics obtained for three different geometries. The response of the short (5×5 m) block remains stable, whereas for the remaining geometries, the ultimate load is reached, after which the global characteristics become unstable. For all the cases considered, the initiation of brittle failure takes place below the ultimate load intensity. The magnitude of the collapse load is certainly influenced by the mechanical characteristics of the interface. It should be pointed out again that the response of both constituent materials (i.e. the intact material and the interface) is assumed to be stable and the instability arises due to the geometric effect of progressive degradation of asperities.

Figure 7 shows the deformed mesh shortly after the ultimate load has been reached. In the 10 m high sample, the failure mechanism involves localization of deformation along two conjugate directions. The deformation mode is symmetric due to the symmetry in

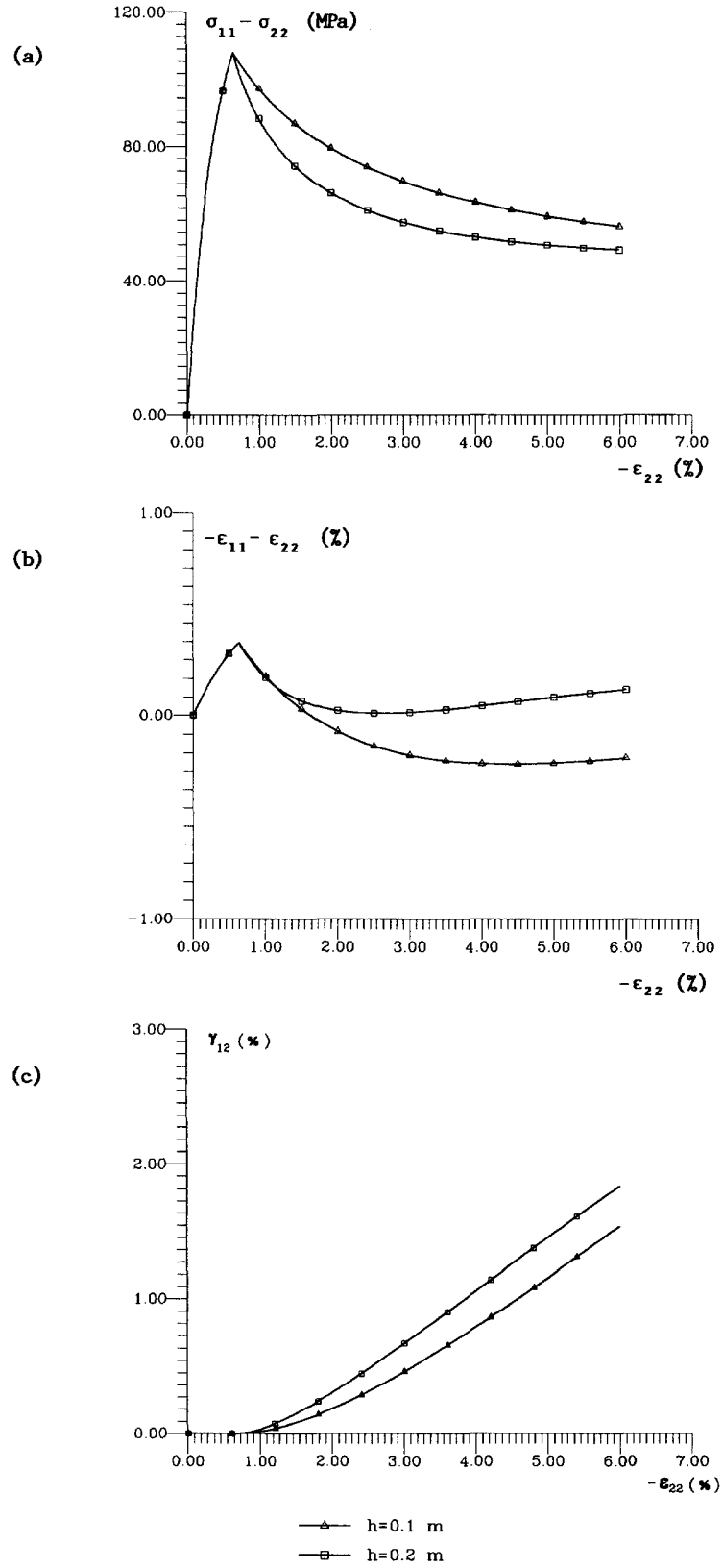

Fig. 5. Influence of the height of the sample on average mechanical characteristics.

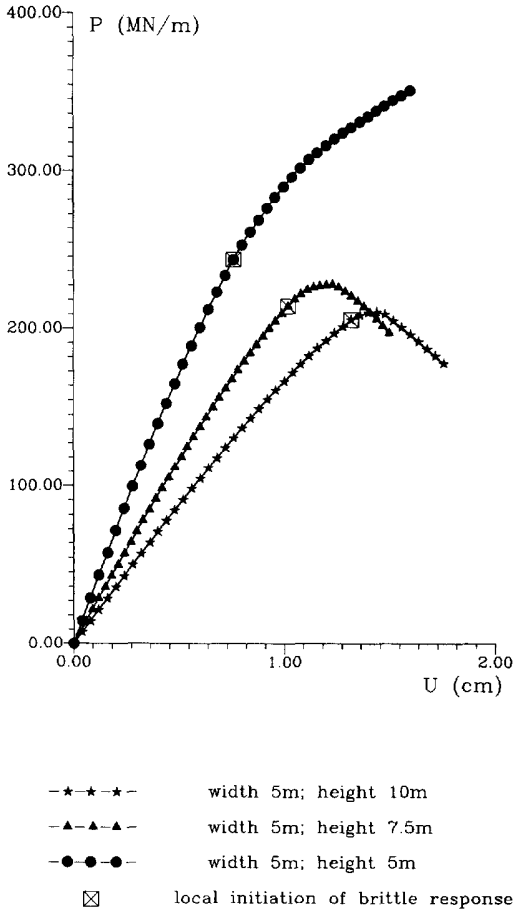

Fig. 6. Load (P)–surface displacement (U) characteristics for concrete blocks subjected to uniaxial compression.

boundary conditions and homogeneity of the material properties. In the short specimen (5×5 m) the predominant mode is the lateral expansion (bulging), with upper and lower parts of the specimen deforming quite uniformly.

FINAL REMARKS

A theoretical framework for the analysis of the mechanical response of plastic-fracturing materials, such as concrete, rocks, ceramic matrix composites, etc., has been presented. It has been assumed that the brittle response, associated with formation of discrete failure planes, is the result of the localization of damage. The onset of localized modes has been considered as a bifurcation problem. The localization criterion has been applied to determine the bifurcation point and the orientation of the failure plane for a series of plane strain uniaxial compression tests performed at different initial confining pressures.

The macroscopic response in the post-localized regime has been estimated based on a homogenization technique. The average properties have been derived from the properties of constituents and the respective volume fractions. A simple, micromechanically-based formulation for the interface behaviour has been discussed, in which the unstable response has been attributed to a progressive degradation of asperities. Numerical examples have been provided, illustrating the influence of confining pressure, as well as that of the geometry of the sample, on the average mechanical response. The results of these simulations are in qualitative agreement with the existing experimental data. The assessment of the quantitative performance, however, requires a comprehensive experimental program involving

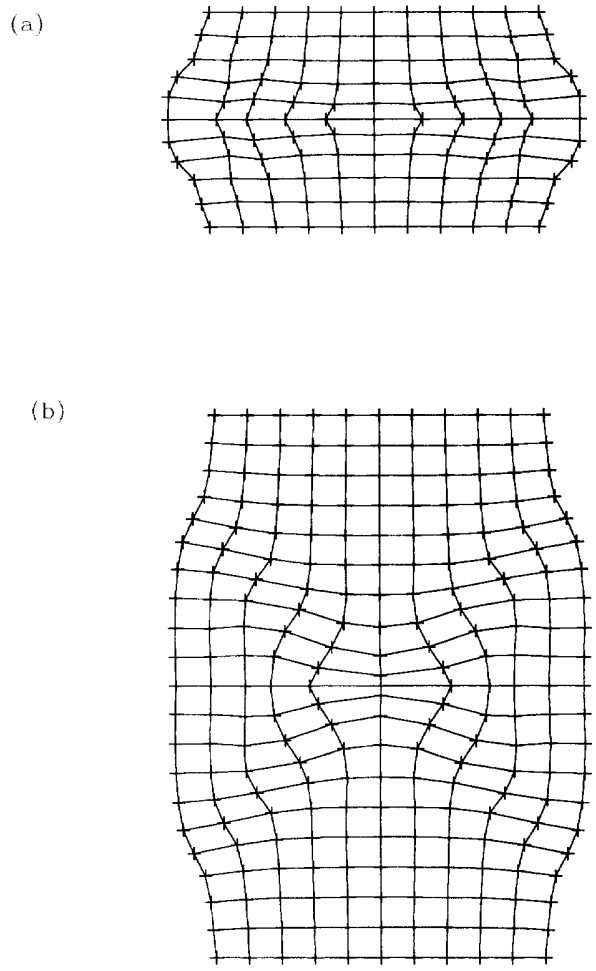

Fig. 7. Deformed mesh: (a) short specimen, 5×5 m; (b) 10×5 m specimen.

the identification of properties of the intact as well as the interface material. Finally, the framework has been implemented in a finite element algorithm to study the response of concrete blocks subjected to uniaxial compression. The objective was to analyse the mode of deformation as a function of the geometry of blocks. The results, which once again should be viewed in qualitative rather than quantitative terms, provide an insight into the mechanism of progressive failure in relation to the load-carrying capacity of the blocks.

REFERENCES

Aifantis, E. C. (1984). On the microstructural origin of certain inelastic models. *J. Engng Mater. Technol.* **106,** 326–334.

Bardet, J. P. (1990). A comprehensive review of strain localization in elastoplastic soils. *Comput. Geotech.* **10,** 163–188.

Bazant, Z. P. (1989). Advances in material modelling of concrete. *10th Int. Conf. on Structural Mechanics in Reactor Technology* (*SMiRT*), Vol. A, pp. 303–329.

de Borst, R. (1991). Simulation of strain localisation: a reappraisal of the Cosserat continuum. *Engng Comput.* **8,** 317–332.

de Borst, R. (1993). A generalization of J_2-flow theory for polar continua. *Comput. Meth. Appl. Mech. Engng* **103,** 347–362.

de Borst, R. and Muhlhaus, H. B. (1992). Gradient-dependent plasticity: formulation and algorithmic aspects. *Int. J. Numer. Meth. Engng* **35,** 521–539.

Dowding, C. H., Zubelewicz, A., O'Connor, K. M. and Belytschko, T. B. (1991). Explicit modelling of dilation, asperity degradation and cyclic seating of rock joints. *Comput. Geotech.* **11,** 209–228.

Dvorak, G. J. and Bahei-El-Din, Y. A. (1982). Plasticity analysis of fibrous composites. *J. Appl. Mech.* **49,** 327–335.

Elfgren, L. (1990). *Fracture Mechanics of Concrete Structures.* Chapman & Hall, London.

Hill, R. (1958). A general theory of uniqueness and stability in elastic plastic solids. *J. Mech. Phys. Solids* **6,** 236–252.
Hill, R. (1963). Elastic properties of reinforced solids; some theoretical principles. *J. Mech. Phys. Solids* **11,** 357–372.
Jiang, J. and Pietruszczak, S. (1988). Convexity of yield loci for pressure sensitive materials. *Comput. Geotech.* **5,** 51–63.
Muhlhaus, H. B. and Aifantis, E. C. (1991). A variational principle for gradient plasticity. *Int. J. Solids Structures* **28,** 845–858.
Muhlhaus, H. B. and Vardoulakis, I. (1987). The thickness of shear bands in granular materials. *Geotechnique* **37,** 271–283.
Ortiz, M. (1987). An analytical study of the localized failure modes of concrete. *Mech. Mater.* **6,** 159–174.
Owen, D. R. J. and Hinton E. (1980). *Finite Elements in Plasticity: Theory and Practice*. Pineridge Press, Swansea.
Palaniswamy, R. and Shah, S. P. (1974). Fracture and stress strain relationship of concrete under triaxial compression. *J. Struct. Div. ASCE* **100**(ST5), 901–916.
Pijaudier-Cabot, G. and Bazant, Z. P. (1987). Nonlocal damage theory. *J. Engng Mech. ASCE* **113,** 1512–1533.
Pietruszczak, S., Jiang, J. and Mirza, F. A. (1988). An elastoplastic constitutive model for concrete. *Int. J. Solids Structures* **24,** 705–722.
Pietruszczak, S. and Krucinski, S. (1989). Description of anisotropic response of clays using a tensorial measure of structural disorder. *Mech. Mater.* **8,** 237–249.
Pietruszczak, S. and Mroz, Z. (1981). Finite element analysis of deformation of strain softening materials. *Int. J. Numer. Meth. Engng* **17,** 327–334.
Pietruszczak, S. and Niu, X. (1993). On the description of localized deformation. *Int. J. Numer. Anal. Meth. Geomech.* **17,** 791–805.
Rudnicki, J. W. and Rice, J. R. (1975). Conditions for the localization of deformation in pressure sensitive dilatant materials. *J. Mech. Phys. Solids* **23,** 371–394.
Sawicki, A. (1983). Engineering mechanics of elastoplastic composites. *Mech. Mater.* **2,** 217–231.
Schneider, H. J. (1976). The friction and deformation behaviour of rock joints. *Rock Mech.* **8,** 170–184.
Thomas, T. Y. (1961). *Plastic Flow and Fracture of Solids*. Academic Press, New York.